Nuclear Engineering and Technology 53 (2021) 1311–1317

Contents lists available at ScienceDirect

Nuclear Engineering and Technology

journal homepage: www.elsevier.com/locate/net

Original Article

Spectral resolution evaluation by MCNP simulation for airborne alpha detection system with a collimator

Min Ji Kim, Si Hyeong Sung, Hee Reyoung Kim*

Nuclear Engineering, Ulsan National Institute of Science and Technology, 50 UNIST-gil, Ulsan, 44919, Republic of Korea

ARTICLE INFO

Article history:
Received 28 February 2020
Received in revised form
10 August 2020
Accepted 14 September 2020
Available online 18 September 2020

Keywords:
Alpha detection
Spectral resolution
Detection efficiency
Monte Carlo simulation

ABSTRACT

In this study, an airborne alpha detection system, which consists of a passivated implanted planar silicon (PIPS) detector and an air filter, was developed. A collimator applied to the alpha detection system showed an enhancement in resolution and a degradation in detection efficiency. The resolution and detection efficiency were compared and analyzed to evaluate the performance of the collimator. Thus, the resolution was found to be more important than the efficiency as a determining factor of the detection system performance, from the viewpoint of radionuclide identification. The performance was evaluated on three properties of the collimator: hole shape, hole length, and the ratio between the hole and frame pitches. From the hole shape performance evaluation, a hexagonal collimator showed the highest resolution. Further, the collimator with a hole pitch of 14 mm was found to have the highest resolution while that with a frame pitch of 4–6 mm (i.e., 1.2–1.4 times longer than the hole pitch) showed the highest resolution.

1. Introduction

Alpha spectrometry is widely used to identify and quantify alpha-particle emitting radionuclides emitted in the decay process. It is also used to analyze radiation measurements in various fields [1–3]. Alpha particles have short ranges and lose energy easily by a high interaction with their medium [4,5]. Owing to these properties, experiments for alpha spectrometry are conventionally conducted in a vacuum or after pretreatment [6,7]. When alpha particles are measured in air in real time, a displacement of the peak occurs in the alpha spectrum due to the loss of alpha energy. This causes spectral distortions due to peak spreading and low-tailing, thus making spectral analysis difficult. Therefore, resolution improvement is essential for analyzing alpha spectra and identifying radionuclides.

The aim of this present study is to develop an airborne alpha detection system. To achieve this, the highly sensitive passivated implanted planar silicon (PIPS) detector was combined with a rolling air filter to collect aerosol samples. In addition, a collimator was added to improve the resolution, and it was placed between the PIPS detector and the air filter where the source was located. Collimation plays an important role in identifying specific radionuclides when multiple radionuclides are collected and measured together in the atmosphere [8–10]. There are two kinds of collimation, namely, the mechanical and electronic collimation [11]. The mechanical collimation is based on a principle that excludes the particles with a certain angle of incidence while the electronic collimation involves the use of voltage pulse distribution on the source electrode or current pulse distribution on the collector electrode [11–13]. In this study, mechanical collimation was considered as electronic collimation is not applicable to PIPS detectors whose detection signals are independent of the incidence angle of radiation.

To evaluate the performance of mechanical collimation, collimators of various shapes and lengths were applied. The alpha detection system was evaluated in the environment of multiple radionuclides including radon (^{222}Rn), thoron (^{220}Rn or ^{220}Th), and their progenies through a Monte Carlo *N*-particle transport code 6 (MCNP6) simulation. The MCNP6 code can simulate several complex geometries and perform transport physics models for criticality, shielding, dosimetry, detector response, and many other applications [14]. The resolution of the detection system was also evaluated by analyzing its full width at half maximum (FWHM) using the ORIGIN software [15]. The changes in resolution and detection efficiency were calculated and compared according to the hole shape and length of the collimator.

* Corresponding author.
E-mail address: kimhr@unist.ac.kr (H.R. Kim).

https://doi.org/10.1016/j.net.2020.09.009

2. Method & materials

2.1. Alpha detection system

A schematic of the detection part of the alpha detection system is shown in Fig. 1. As a roller rotates, the alpha-emitting radionuclides collected in the air filter are measured by the PIPS detector, which is effective for alpha particle detection due to its high sensitivity. PIPS detectors have various resolutions and detection efficiencies depending on the active area. The resolutions of PIPS detector vary from 34–38 keV to 55–70 keV in vacuum. The PIPS450 model, which has the highest resolution of 34–38 keV among the Canberra CAM PIPS detectors series [16], was used to simulate the performance of the alpha detection system.

The PIPS450 has a diameter of 23.9 mm, an active area of 450 mm^2, and a height of 12.3 mm. The air filter composed of a cellulose-asbestos paper, which has a diameter of 50 mm and a thickness of 0.2 mm, is located 2 cm away from the PIPS detector as seen in Fig. 1. The collimator is located between the PIPS detector and air filter as seen in Figs. 1 and 2. The shielding box with a thickness of 2 mm, which blocks natural radiation, surrounds the detector, filter and collimator, and it is made of stainless steel 304. The remaining space contains air. A schematic of the alpha detection system for simulation is shown in Fig. 2.

2.2. The principle of collimation

A schematic of the incidence of alpha particles on the PIPS detector is shown in Fig. 3. In Fig. 3 (a), particles 1, 2, and 3 all enter the detector in air. However, particle 3, which has a larger angle of incidence, travels a longer distance to reach the detector as seen in Fig. 3(a). This causes a considerable low-tailing at the low-energy part of the alpha spectrum due to the energy loss. Thus, the particles with large angles of incidence shift the energy peak to the left and cause resolution degradation due to the low-tailing.

A collimator prevents particles with a large angle of incidence such as particle 3 from entering the detector. In Fig. 3 (b), particles 4 and 5 with small angles of incidence enter the detector, while particle 6 with a larger angle of incidence is blocked by the collimator from entering the PIPS detector. In other words, by applying the collimator in front of the detector, alpha particles, which lose considerable energy, with a large incident angle do not enter the detector, leading to less low-tailing. Thus, the collimator makes the detection efficiency decrease as fewer particles are incident on the detector while it improves the resolution due to a less energy shift.

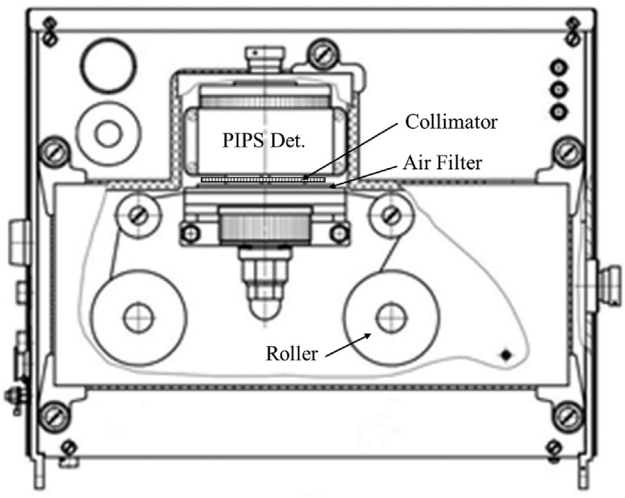

Fig. 1. Schematic representation of the detection part of alpha detection system.

2.3. Collimator

The collimator was set as a cuboid with a length of 6 cm, width of 6 cm, and height of 1 cm, and it was located 0.5 cm away from the air filter and the PIPS detector, as shown in Fig. 2. The frame of the collimator was made of aluminum, and the hole comprised air, that is, empty space.

When using a collimator to improve the resolution, hexagonal and tetragonal collimators are generally used [17], where the hexagonal collimators are regarded as the most effective in terms of resolution [18]. Additionally, tetragonal collimators with rectangular holes may have a higher resolution [19]. Moreover, circular collimators are further evaluated. To evaluate the performance of the collimator in this study, changes in resolution and detection efficiency were compared and analyzed on three hole shapes such as hexagonal, circular, and tetragonal shapes. The hexagonal and circular collimators have a hexagonal prism triangle lattice, and the tetragonal collimator has a hexahedron square lattice, as shown in Fig. 4. The three collimator designs according to hole shape are shown in Fig. 4. The number and diameter of holes were set equal for comparisons according to changes in hole length. The size and number of the hexagonal collimator were set first. Subsequently, the size and number of the circular and tetragonal ones were determined accordingly. The length of hole for all collimators was set as 16 mm, and the number of holes was set as nine. The performance was also evaluated for various hole lengths of collimators. For the length of the collimators, the three collimators have different meanings. First, the length of the hexagonal one means a pitch, that is, the length between sides [20]. The length of one side (r) and the pitch (p) have a relationship of $p = \sqrt{3} \times r$, as shown in Fig. 5 (a). In addition, the length of the circular one means a diameter while the length of the tetragonal one means that of one side. These lengths were the criterion for performance evaluation according to hole length. The considered lengths were 7 cases of 10 mm, 12 mm, 14 mm, 16 mm, 18 mm, 20 mm, and 22 mm. Furthermore, the resolution and detection efficiency of the collimators were evaluated according to the change of holes and frame lengths. The hole and frame length (or pitch) are illustrated in Fig. 5 (b).

2.4. Monte Carlo simulation

A general-purpose Monte Carlo code, MCNP6, was used to evaluate the collimation performance. The MCNP6 code can be used in transport physics models for criticality, shielding, dosimetry, and detector response. The code can also be used in several other applications that simulate several complex geometries and track several particle types over broad ranges of energies [14] as the geometry card for the detector system with a collimator is modeled in Fig. 2 (a) and (b) for the simulation. The geometry is described in detail in Sections 2.1 and 2.3.

The sources are emitted from the air filter isotropically towards the detector. The sources considered were polonium radioisotopes of ^{218}Po, ^{214}Po, ^{212}Po, and ^{210}Po, which show the energy clearly distinguished among the radon (^{222}Rn) and thoron (^{220}Rn or ^{220}Th) progenies [21], and having the peak energy of the spectrum with 6.002 MeV, 7.687 MeV, 8.784 MeV, and 5.304 MeV, respectively. A physical model F8 tally and a Gaussian energy broadening (GEB) function provide alpha spectra. Thus, the F8 tally and GEB function were used to calculate the pulse-height value for detection efficiency and to perform the simulation of the resolution from the spectra, respectively.

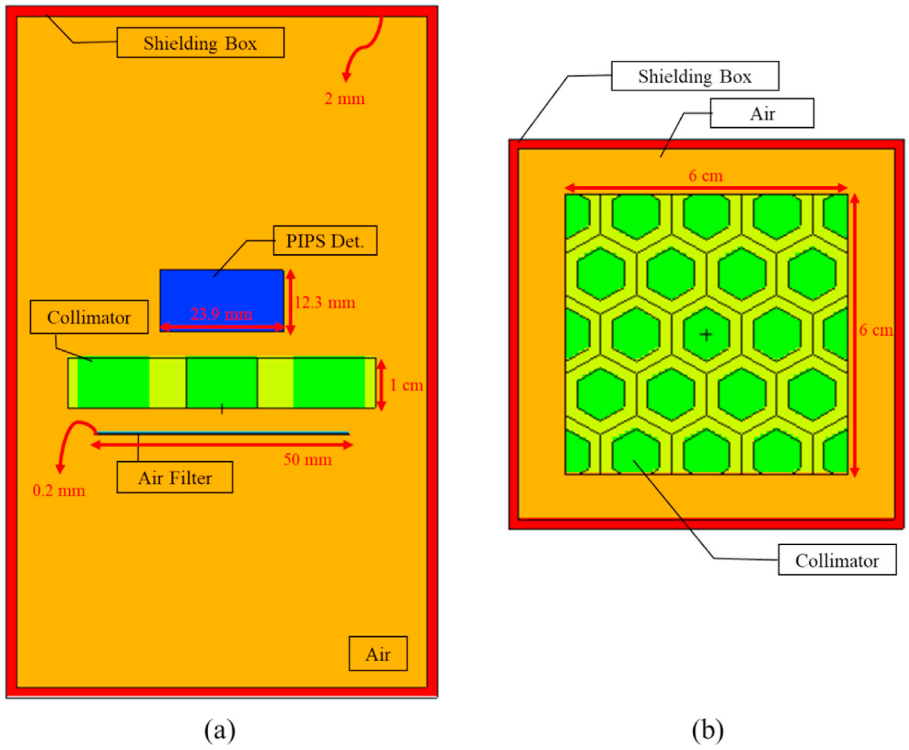

Fig. 2. Schematic representation of alpha detection system for simulation ((a) longitudinal section and (b) cross-section of the collimator).

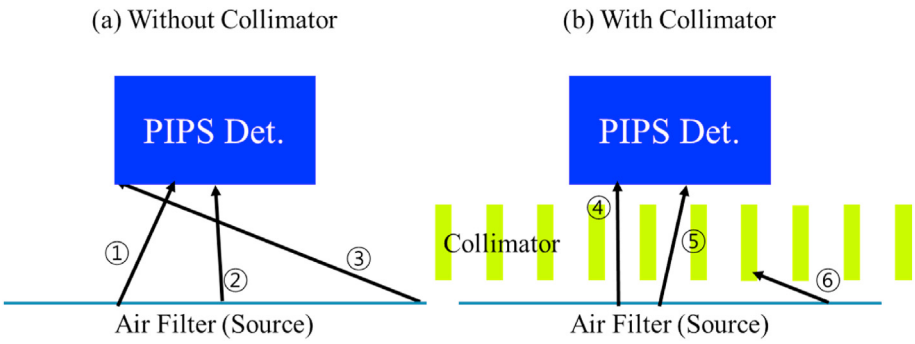

Fig. 3. Schematic representation of the incidence of alpha particles into PIPS detector, ((a) without collimator and (b) with collimator).

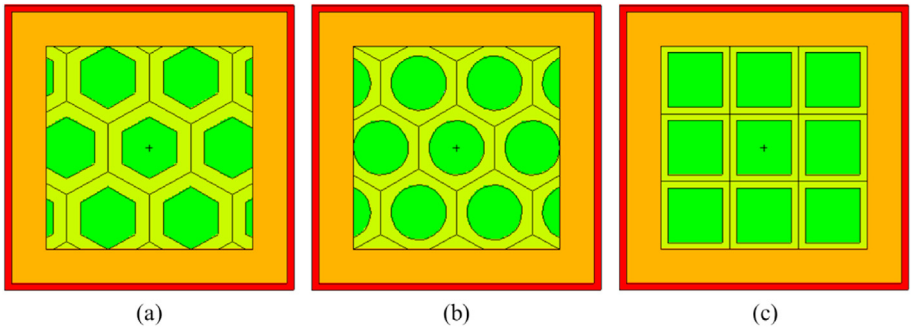

Fig. 4. Collimator designs according to the hole shapes, ((a) hexagonal collimator, (b) circular collimator, and (c) tetragonal collimator).

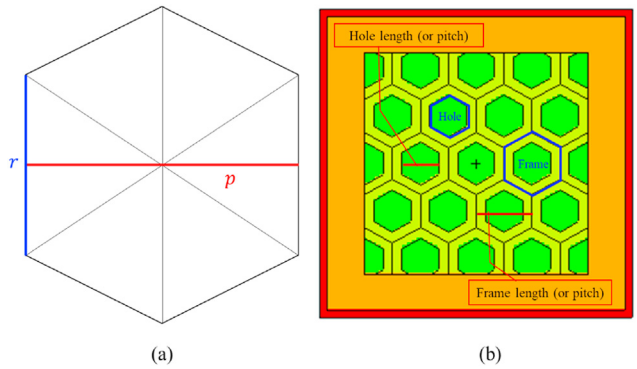

Fig. 5. Diagram of the length for the hexagonal collimator ((a) Relationship between the length of one side and the pitch and (b) definition of hole and frame length (or pitch)).

3. Results and discussion

3.1. Hole shape of collimator

The spectra on the collimators with three holes of hexagonal, circular, and tetragonal shapes are shown in Fig. 6, and the resolution and detection efficiency for the collimators are shown in Table 1. The FWHM value was expressed as the average value of those on four peaks, which include ^{218}Po (6.002 MeV), ^{214}Po (7.687 MeV), ^{212}Po (8.784 MeV), and ^{210}Po (5.304 MeV). The circular collimator had an FWHM of 192.7 keV and a detection efficiency of 0.922%. The tetragonal collimator had a lower resolution of 195.5 keV and a higher detection efficiency of 1.31% than the circular one as shown in Table 1. The hexagonal collimator had a resolution of 189.6 keV and a detection efficiency of 0.999%. The hexagonal collimator showed an 8.33% higher detection efficiency due to its close-packed lattice and a 1.62% higher resolution compared to the circular one. Furthermore, the hexagonal collimator showed a 24.1% lower detection efficiency and a 3.01% higher resolution than the tetragonal one. The FWHM value of each peak had 5–12% difference from the average FWHM value for the hexagonal collimator.

As explained in Section 2.2, the angle of incidence determines whether the particles enter the detector, thus the importance of the hole length. Even if the hole length is fixed, the length varies depending on the point of measurement. That is, although the hole length of a tetragonal collimator means the length of a side is 16 mm, the diagonal length of the tetragonal collimator is $16\sqrt{2}$ mm, a slightly different value. Therefore, the resolution and detection efficiency vary depending on the hole shape of the collimators.

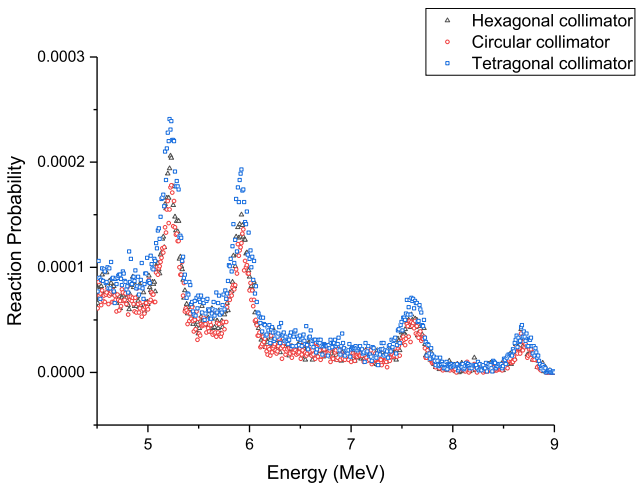

Fig. 6. Spectrum graph according to the shape of hole of collimator.

The hole shape of an ideal collimator was thought to be hexagonal when it had the same length as the holes in terms of resolution. Although the degradation of detection efficiency is greater than the improvement of resolution, using the collimator would be advantageous in the actual monitoring environment, considering that the resolution improvement is a significant factor in terms of radionuclide identification. Thus, the collimator of hexagonal hole, which had the smallest FWHM value, was thought to be the most suitable, leading to the best performance of the alpha detector system.

3.2. Hole length (or pitch) of collimator

The analysis of the collimator's hole shape showed that the hexagonal shape had the highest resolution in Section 3.1. Thus, the hexagonal collimator was evaluated for resolution and detection efficiency according to the hole length (or pitch). The considered hole pitches of the hexagonal collimator were 10 mm, 12 mm, 14 mm, 16 mm, 18 mm, 20 mm, and 22 mm, where the frame pitch of the collimator was set 1.5 times as long as each hole pitch for consistency, as shown in Table 2.

The spectra according to the hole pitch of the collimator are shown in Fig. 7, and the resolution and detection efficiency according to hole pitch are shown in Table 2. When the hole pitch decreased from 22 mm to 14 mm, the detection efficiency decreased from 1.623% to 0.780% while the FWHM value decreased from 196.2 keV to 185.0 keV. The collimator with smaller holes had a lower detection efficiency as fewer particles entered the detector. Hence, the smaller the hole size of collimator, the fewer the incidence of alpha particles with a large angle of incidence, leading to less energy shift due to the reduction of low-tailing. Consequently, the FWHM value was smaller.

However, when the hole pitch decreased from 14 mm to 10 mm, the detection efficiency increased from 0.780% to 0.907% while the FWHM value increased from 185.0 keV to 200.7 keV. As expected in the case of considerably smaller collimator holes, the alpha particles reaching the end of the collimator caused more low-tailing due to scattering, resulting in a slightly larger FWHM value. The low-tailing for low alpha energy occurred more than that for high alpha energy. Therefore, the collimator with a hole pitch of 14 mm had the smallest FWHM value of 185.0 keV but produced the highest resolution. The FWHM value of each peak had 1–12% difference from the average FWHM value for the collimator with a hole pitch of 14 mm.

3.3. Hole and frame pitch of collimator

As explained in Section 3.2, the larger the hole of the collimator, the higher the detection efficiency when the hole pitch is larger than 14 mm. For each hole area of the collimator, the larger the hole, the smaller the frame. In other words, the longer the hole pitch and the shorter the frame pitch, the higher the detection efficiency. The detection efficiencies according to change of hole and frame pitch are shown in Table 3. The average detection efficiency of the collimator with a hole pitch of 14 mm was 1.16%, while the average detection efficiency of the collimator with a hole pitch of 20 mm was 1.47%. That is, as the hole pitch of the collimator increased, the detection efficiency also increased. In addition, as the frame pitch increased, the detection efficiency decreased at each

Table 1
Resolution and detection efficiency according to the hole shape of collimator.

	Circular Collimator	Tetragonal Collimator	Hexagonal Collimator
Length of hole [mm]	16	16	16
Average FWHM [keV]	192.7 ± 8.167	195.5 ± 17.01	189.6 ± 17.09
Detection Efficiency [%]	0.922 ± 0.00144	1.31 ± 0.00191	0.999 ± 0.00150

Table 2
Resolution and detection efficiency according to the hole pitch of collimator.

	Pitch_10	Pitch_12	Pitch_14	Pitch_16	Pitch_18	Pitch_20	Pitch_22
Hole pitch [mm]	10	12	14	16	18	20	22
Frame pitch [mm]	15	18	21	24	27	30	33
Average FWHM [keV]	200.2 ±12.77	187.9 ±7.757	185.0 ±15.69	190.3 ±15.53	195.1 ±18.52	202.2 ±18.01	196.2 ±14.47
Detection Efficiency [%]	0.907 ±0.00132	0.839 ±0.00123	0.780 ±0.00116	0.897 ±0.00137	1.08 ±0.00161	1.27 ±0.00182	1.62 ±0.00194

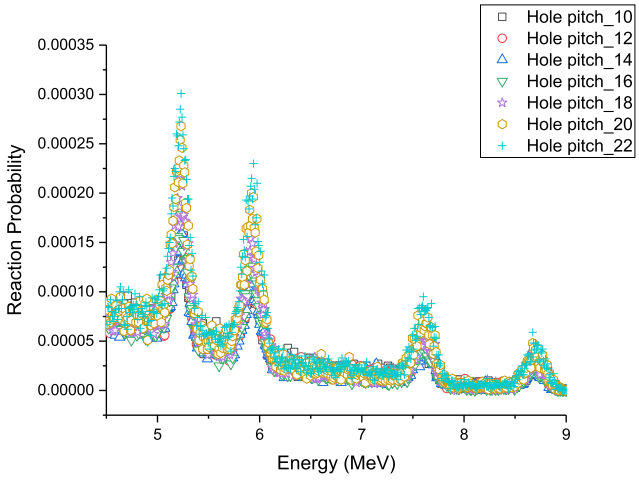

Fig. 7. Spectrum graph according to the hole pitch of collimator.

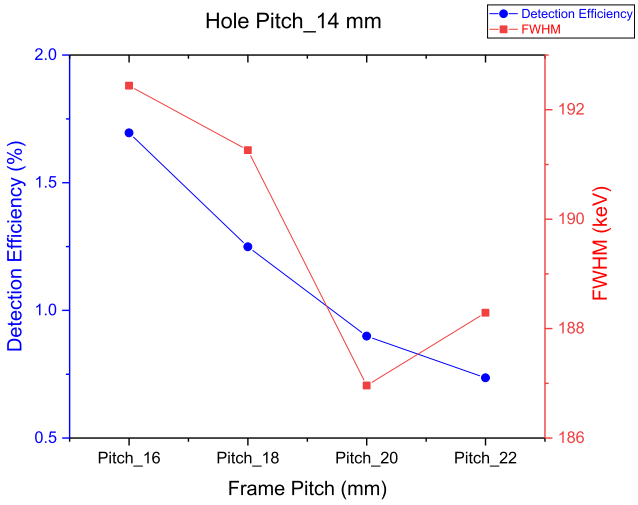

Fig. 8. Change in detection efficiency and resolution according to the change in frame pitch in case of a collimator with the hole pitch of 14 mm.

hole pitch. Using the collimator with a hole pitch of 14 mm as an example, the detection efficiency decreased from 1.70% to 0.736% as the frame pitch increased from 16 mm to 22 mm, as shown in Fig. 8. Changes in detection efficiency and resolution according to change in frame pitch in the collimator with a hole pitch of 14 mm are shown in Fig. 8.

The resolution according to the change of hole and frame pitch are shown in Table 4. The resolution degraded as shown in Table 4, that is, the FWHM value increased, as the hole pitch increased. The result of the resolution was different than that of the detection

Table 3
Detection efficiency according to the ratio between hole and frame pitch of collimator.

Detection efficiency [%]		Hole pitch [mm]			
		Pitch_14	Pitch_16	Pitch_18	Pitch_20
Frame pitch [mm]	Pitch_16	1.70 ±0.00218	–	–	–
	Pitch_18	1.25 ±0.00175	1.71 ±0.00218	–	–
	Pitch_20	0.899 ±0.00136	1.26 ±0.00180	1.75 ±0.00229	–
	Pitch_22	0.736 ±0.00115	0.999 ±0.00150	1.35 ±0.00196	1.78 ±0.00235
	Pitch_24	–	0.897 ±0.00137	1.15 ±0.00172	1.47 ±0.00213
	Pitch_26	–	–	1.10 ±0.00166	1.31 ±0.00187
	Pitch_28	–	–	–	1.30 ±0.00188

Table 4
Resolution according to the ratio between hole and frame pitch of collimator.

FWHM [keV]		Hole pitch [mm]			
		Pitch_14	Pitch_16	Pitch_18	Pitch_20
Frame pitch [mm]	Pitch_16	192.4 ±14.76	–	–	–
	Pitch_18	191.3 ±13.31	193.9 ±18.23	–	–
	Pitch_20	187.0 ±13.48	190.3 ±13.77	196.1 ±19.45	–
	Pitch_22	188.3 ±12.63	189.6 ±17.09	191.6 ±16.05	206.0 ±18.95
	Pitch_24	–	190.3 ±15.53	193.2 ±16.82	201.7 ±16.83
	Pitch_26	–	–	195.6 ±17.23	199.1 ±18.41
	Pitch_30	–	–	–	202.4 ±17.85

efficiency. At each hole pitch of the collimator, as the frame pitch increased, the FWHM value decreased and then increased from a specific frame pitch. The alpha particles blocked by the hole are the same at a constant hole pitch. However, if the frame is too large, alpha particles that can fully enter would not enter the detector. Consequently, the reaction probability decreases, and the resolution is not improved. In Table 4 and Fig. 8, considering the collimator with a hole pitch of 14 mm, it is observed that the FWHM value decreases from 192.4 keV to 187.0 keV as the frame pitch increases from 16 mm to 20 mm but increases to 188.3 keV at the frame pitch of 22 mm. The FWHM value of each peak had 1–10% difference from the average FWHM value for the collimator with a hole pitch of 14 mm. In addition, the detection efficiency decreased as the hole pitch decreased at each frame pitch. The combinations of hole pitch and frame pitch that had the lowest FWHM value were (14, 20), (16, 22), (18, 22), and (20, 26). In other words, when the frame pitch was about 4–6 mm longer than the hole pitch or approximately 1.2–1.4 times longer than the hole pitch, the FWHM value was the smallest, which provided the highest resolution at each hole pitch.

4. Conclusion

In this study, the performance of collimators was evaluated using MCNP6 code to develop an airborne alpha detection system with a high resolution. The evaluation showed that the hexagonal collimator had the highest resolution among the three hole shapes of the collimators. For the fixed ratio between the hole pitch and frame pitch of the collimator, the highest resolution had 185.0 keV of FWHM at a 14 mm hole pitch. The change of hole and frame pitch showed that the highest resolution could be determined in spite of efficiency degradation. It was seen that the highest resolution occurred when the frame pitch was 4–6 mm or 1.2–1.4 times longer than the hole pitch.

The collimator was believed to improve spectral analysis of the airborne alpha detection system. The application of the optimized collimator in an actual measurement environment is expected to provide higher spectra resolutions in terms of radionuclide identification.

Declaration of competing interest

The authors declare that they have no known competing financial interests or personal relationships that could have appeared to influence the work reported in this paper.

Acknowledgments

This work was supported by the National Research Foundation of Korea (NRF) grant funded by the Korean government (MSIP: Ministry of Science, ICT and Future Planning) NRF-22A20153413555, This work was supported by the 'Development of Portable Radioactive Contamination Monitoring System for Alpha and Beta Dust Source in the Air' of the Korea Institute of Energy Technology Evaluation and Planning(KETEP) granted financial resource from the Ministry of Trade, Industry & Energy, Republic of Korea (No. 20171510300590).

References

[1] E. García-Toraño, Current status of alpha-particle spectrometry, Appl. Radiat. Isot. 64 (10–11) (2006) 1273–1280.
[2] R. Pöllänen, Performance of an in-situ alpha spectrometer, Appl. Radiat. Isot. 109 (2016) 193–197.
[3] K.M. Glover, Alpha-particle spectrometry and its applications, Int. J. Appl. Radiat. Isot. 35 (4) (1984) 239–250.
[4] P. Martin, G.J. Hancock, Peak resolution and tailing in alpha-particle spectrometry for environmental samples, Appl. Radiat. Isot. 61 (2–3) (2004) 161–165.
[5] E. Holm, Review of alpha-particle spectrometric measurements of actinides, Int. J. Appl. Radiat. Isot. 35 (4) (1984) 285–290.
[6] P. De Regge, R. Boden, Review of chemical separation techniques applicable to alpha spectrometric measurements, Nucl. Instrum. Methods Phys. Res. 223 (2–3) (1984) 181–187.
[7] J.S. Alvarado, K.A. Orlandini, M.D. Erickson, Rapid determination of radium isotopes by alpha spectrometry, J. Radioanal. Nucl. Chem. 194 (1) (1995) 163–172.
[8] R. Pöllänen, K. Peräjärvi, T. Siiskonen, J. Turunen, In-situ alpha spectrometry from air filters at ambient air pressure, Radiat. Meas. 53 (2013) 65–70.
[9] D.A. Pripachkin, D.V. Aron, A.K. Budyka, Y.N. Khusein, Collimator effect on semiconductor α-spectrometer characteristics in measurements of radioactive aerosols, Atom. Energy 125 (2) (2018) 119–123.
[10] R.A. Wolfe, W.F. Stubbins, A neutron spectrometer employing charged-particle collimation to improve resolution, Nucl. Instrum. Methods 60 (3) (1968) 246–252.
[11] S. Park, S.W. Kwak, H.B. Kang, High resolution alpha particle spectrometry through collimation, Nucl. Instrum. Methods Phys. Res. Sect. A Accel. Spectrom. Detect. Assoc. Equip. 784 (2015) 470–473.
[12] D.W. Engelkemeir, L.B. Magnusson, Resolution of alpha-particle spectra by ionization pulse analysis of collimated samples, Rev. Sci. Instrum. 26 (3) (1955) 295–302.
[13] R. Benoit, G. Bertolini, G.B. Restelli, Collimation of alpha particles in an ionization chamber, Nucl. Instrum. Methods 29 (1) (1964) 149–156.
[14] MCNP User's Manual Code Version 6.2. LA-UR-17-29981, Los Alamos National Laboratory Report, California, 2017.
[15] Origin User Guide, OriginLab Corporation, USA, 2016.
[16] The Continuous Air Monitoring (CAM) PIPS® Detector Properties and Applications, Application Note, Canberra Industry, U.S.A, 2011.
[17] D.J. de Vries, S.C. Moore, Comparison of hexagonal-hole and square-hole collimation by Monte Carlo simulation, in: 2000 IEEE Nuclear Science Symposium. Conference Record (Cat. No. 00CH37149), vol. 3, IEEE, 2000, pp. 22–52.

[18] R. Pöllänen, K. Peräjärvi, T. Siiskonen, J. Turunen, High-resolution alpha spectrometry at ambient air pressure – towards new applications, Nucl. Instrum. Methods Phys. Res. Sect. A Accel. Spectrom. Detect. Assoc. Equip. 695 (2012) 173–178.
[19] Y.J. Lee, H.J. Ryu, H.M. Cho, S.W. Lee, Y.N. Choi, H.J. Kim, Optimization of an ultra-high-resolution parallel-hole collimator for CdTe semiconductor SPECT system, J. Instrum. 8 (1) (2013), C01044.
[20] MCNP Extensions Version 2.5.0. LA-UR-05-2675, Los Alamos National Laboratory, California, 2005.
[21] R.B. Hayes, Continuous air monitor algorithm development, Nucl. Technol. 168 (1) (2009) 35–40.